

Lead-tellurium oxysalts from Otto Mountain near Baker, California: XI. Eckhardite, $(\text{Ca,Pb})\text{Cu}^{2+}\text{Te}^{6+}\text{O}_5(\text{H}_2\text{O})$, a new mineral with HCP stair-step layers

ANTHONY R. KAMPF,^{1,*} STUART J. MILLS,² ROBERT M. HOUSLEY,³ GEORGE R. ROSSMAN,³
JOSEPH MARTY,⁴ AND BRENT THORNE⁵

¹Mineral Sciences Department, Natural History Museum of Los Angeles County, 900 Exposition Boulevard, Los Angeles, California 90007, U.S.A.

²Geosciences, Museum Victoria, GPO Box 666, Melbourne 3001, Victoria, Australia

³Division of Geological and Planetary Sciences, California Institute of Technology, Pasadena, California 91125, U.S.A.

⁴5199 E. Silver Oak Road, Salt Lake City, Utah 84108, U.S.A.

⁵3898 S. Newport Circle, Bountiful, Utah 84010, U.S.A.

ABSTRACT

Eckhardite, $(\text{Ca,Pb})\text{Cu}^{2+}\text{Te}^{6+}\text{O}_5(\text{H}_2\text{O})$, is a new tellurate mineral from Otto Mountain near Baker, California, U.S.A. It occurs in vugs in quartz in association with Br-rich chlorargyrite, gold, housleyite, khinite, markcooperite, and ottoite. It is interpreted as having formed from the partial oxidation of primary sulfides and tellurides during or following brecciation of quartz veins. Eckhardite is monoclinic, space group $P2_1/n$, with unit-cell dimensions $a = 8.1606(8)$, $b = 5.3076(6)$, $c = 11.4412(15)$ Å, $\beta = 101.549(7)^\circ$, $V = 485.52(10)$ Å³, and $Z = 4$. It forms as needles or blades up to about $150 \times 15 \times 5$ µm in size, typically in radial or sub-radial aggregates, but also as isolated needles. The color is light bluish green and the streak is very pale bluish green. Crystals are transparent with vitreous to subadamantine luster. The Mohs hardness is estimated at between 2 and 3. Eckhardite is brittle with an irregular fracture and one likely (but not observed) cleavage on $\{101\}$. The calculated density based on the empirical formula is 4.644 g/cm³. The mineral is biaxial (–), with indices of refraction of $\alpha = 1.770$ (calc), $\beta = 1.860$ (calc), and $\gamma = 1.895(5)$. The measured $2V$ is $61.2(5)^\circ$, dispersion is $r < v$, perceptible and the optical orientation is $Z = \mathbf{b}$; $X \approx [101]$. The pleochroism is: Z (light blue green) $< Y$ (very pale blue green) $< X$ (colorless). The normalized electron microprobe analyses (average of 4) provided: PbO 4.79, CaO 15.90, MgO 0.06, CuO 22.74, Fe₂O₃ 0.06, TeO₃ 51.01, H₂O 5.45 (structure), total 100 wt%. The empirical formula (based on 6 O apfu) is: $\text{Ca}_{0.962}\text{Pb}_{0.073}\text{Cu}_{0.971}^{2+}\text{Mg}_{0.005}\text{Fe}_{0.002}^{3+}\text{Te}_{0.986}^{6+}\text{O}_6\text{H}_{2.052}$. The Raman spectrum exhibits prominent features consistent with the mineral being a tellurate, as well as an OH stretching feature confirming a hydrous component. The eight strongest powder X-ray diffraction lines are [d_{obs} in Å (hkl) I]: 5.94 (101) 100, 3.287 (112) 80, 2.645 (020, $\bar{2}13$) 89, 2.485 ($\bar{1}14, 301, 014$) 48, 2.245 (114, 122) 46, 1.809 (223, $\bar{4}13, 321, \bar{4}04$) 40, 1.522 (413, $\bar{5}12, 421, 133$) 42, and 1.53 ($\bar{2}17, \bar{2}33, \bar{4}06$) 43. The crystal structure of eckhardite ($R_1 = 0.046$ for 586 reflections with $F_o > 4\sigma F$) consists of stair-step-like octahedral layers of Te^{6+}O_6 and Cu^{2+}O_6 octahedra parallel to $\{101\}$, which are linked in the $[10\bar{1}]$ direction by bonds to interlayer Ca atoms. The structure can be described as a stacking of stepped HCP layers alternating with chains of CaO_7 polyhedra. The structures of bairdite, timroseite, and paratimroseite also contain stair-step-like HCP polyhedral layers.

Keywords: Eckhardite, new mineral, tellurate, crystal structure, Raman spectroscopy, HCP layers, bairdite, timroseite, paratimroseite, Otto Mountain, California

INTRODUCTION

Eckhardite is the twelfth new mineral (Table 1) to be described from the remarkable Pb-Cu-Te-rich secondary mineral assemblage at Otto Mountain near Baker, California, U.S.A. (Kampf et al. 2010a; Housley et al. 2011). Eckhardite is named for Colonel Eckhard D. Stuart (born 1939) of Madison, Mississippi, U.S.A. Stuart was a member of the General Staff of the West German Army until retiring in 1986. He then moved to the United States where he worked for the BASF Corporation for 10 years while taking courses in geology and chemistry at Fairley Dickinson and Duke Universities. He began collecting minerals in 1988, specializing in field-collecting, mainly in the Western United States. Stuart has developed an excellent eye for

unusual micro-species. He has submitted numerous phases for scientific study, including several potentially new species. The co-type specimen of eckhardite that yielded the crystals used in the structure determination and EMPA was collected by Stuart, who provided it for study. Stuart has agreed to the naming of the mineral in his honor. His first name is employed because the pronunciation of the name “stuartite” would be the same as that of the existing mineral stewartite and the compound name “eckhardstuartite” is clearly more awkward.

The new mineral and name have been approved by the Commission on New Minerals, Nomenclature and Classification of the International Mineralogical Association (IMA 2012-085). Two co-type specimens are deposited in the Natural History Museum of Los Angeles County under catalog numbers 62512 and 64011. The first of these was collected by one of the authors (B.T.) at the Bird Nest drift on Otto Mountain and is also one

* E-mail: akampf@nhm.org

TABLE 1. New minerals described from Otto Mountain

Mineral	Ideal formula	Reference
Ottoite	$\text{Pb}_2\text{Te}^{6+}\text{O}_5$	Kampf et al. (2010a)
Housleyite	$\text{Pb}_2\text{Cu}^{2+}\text{Te}_4^{6+}\text{O}_{18}(\text{OH})_2$	Kampf et al. (2010b)
Thorneite	$\text{Pb}_6(\text{Te}^{6+}\text{O}_{10})(\text{CO}_3)\text{Cl}_2(\text{H}_2\text{O})$	Kampf et al. (2010c)
Markcooperite	$\text{Pb}_2(\text{UO}_2)\text{Te}^{4+}\text{O}_6$	Kampf et al. (2010d)
Timroseite	$\text{Pb}_2\text{Cu}_2^{2+}(\text{Te}^{6+}\text{O}_6)_2(\text{OH})_2$	Kampf et al. (2010e)
Paratimroseite	$\text{Pb}_2\text{Cu}_2^{2+}(\text{Te}^{6+}\text{O}_6)_2(\text{H}_2\text{O})_2$	Kampf et al. (2010e)
Telluroperite	$\text{Pb}_2\text{Te}^{4+}\text{O}_4\text{Cl}_2$	Kampf et al. (2010f)
Chromschiefelinite	$\text{Pb}_{10}\text{Te}_8^{6+}\text{O}_{20}(\text{CrO}_4)(\text{H}_2\text{O})_5$	Kampf et al. (2012)
Fuetererite	$\text{Pb}_3\text{Cu}_8^{2+}\text{Te}_6^{6+}\text{O}_6(\text{OH})_7\text{Cl}_5$	Kampf et al. (2013a)
Agaitite	$\text{Pb}_2\text{Cu}^{2+}\text{Te}^{6+}\text{O}_5(\text{OH})_2(\text{CO}_3)$	Kampf et al. (2013b)
Bairdite	$\text{Pb}_2\text{Cu}_2^{2+}\text{Te}_2^{6+}\text{O}_{10}(\text{OH})_2(\text{SO}_4)(\text{H}_2\text{O})$	Kampf et al. (2013c)
Eckhardite	$(\text{Ca,Pb})\text{Cu}^{2+}\text{Te}^{6+}\text{O}_5(\text{H}_2\text{O})$	This study

of the co-types for markcooperite (Kampf et al. 2010d). The second was collected by Eckhard Stuart at the Aga mine, also on Otto Mountain.

OCCURRENCE

The Aga mine is located at 35.27215°N, 116.09487°W at an elevation of 1055 feet on Otto Mountain, 1 mile northwest of Baker, San Bernardino County, California. The Bird Nest drift is located at 35.27677°N, 116.09927°W on the southwest flank of Otto Mountain, 0.4 miles northwest of the Aga mine.

Eckhardite is relatively rare at both sites. The description is based upon the two co-type specimens noted above, both of which are <2 cm in maximum dimension; however, we are aware of several other specimens that have been found by collectors. Crystals occur in vugs in quartz in association with Br-rich chlorargyrite, gold, housleyite, khinite, markcooperite, and ottoite. Other species identified in the mineral assemblages at Otto Mountain include acanthite, agaite, anglesite, anatacamite, atacamite, bairdite, boleite, brochantite, burckhardtite, calcite, caledonite, celestine, cerussite, chalcopryrite, chromschiefelinite, chrysocolla, devilline, diaboite, eztlite, fluorite, fornacite, frankhawthorneite, fuetererite, galena, goethite, hematite, hessite, iodargyrite, jarosite, kuranakhite, linarite, malachite, mattheddleite, mcalpinite, mimetite, mottramite, munakataite, murdochite, muscovite, paratimroseite, perite, phosphohedyphane, plumbojarosite, plumbotsumite, pyrite, telluroperite, thorneite, timroseite, vanadinite, vauquelinite, wulfenite, and xocomecatlite.

Eckhardite is a secondary oxidation zone mineral and is presumed to have formed by oxidation of tellurides, chalcopryrite, and galena. Notably, eckhardite is one of only six phases thus far identified in the Otto Mountain mineral assemblage that contain essential Ca (the others being calcite, devilline, fluorite, gypsum, and phosphohedyphane) and it is the only tellurate in the assemblage containing essential Ca. As explained in the crystal structure section, the Ca site contains a small, but significant, content (7–9%) of Pb. Additional background on the occurrence is provided in Kampf et al. (2010a) and Housley et al. (2011).

PHYSICAL AND OPTICAL PROPERTIES

Eckhardite occurs as needles or blades elongated on [010] and sometimes flattened on {101}, up to about $150 \times 15 \times 5 \mu\text{m}$ in size. Crystals typically are grouped in radial or sub-radial aggregates, but also are found as isolated needles (Figs. 1 and 2). Forms observed are {101}, {10 $\bar{1}$ }, and {011} (Fig. 3). No twinning was observed optically under crossed polars or based upon single-crystal X-ray diffraction. The color is light bluish green and

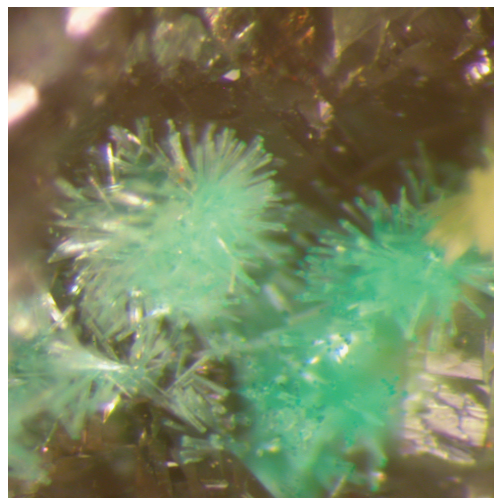


FIGURE 1. Crystals of eckhardite on quartz from the Bird Nest drift. FOV 0.5 mm. Brent Thorne specimen. (Color online.)

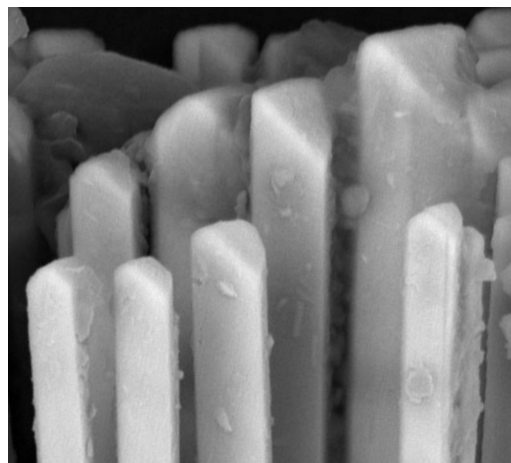


FIGURE 2. SEM image showing the {011} terminations of eckhardite needles.

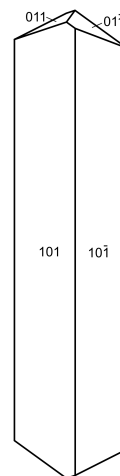


FIGURE 3. Crystal drawing of eckhardite (clinographic projection in nonstandard orientation, *b* vertical).

the streak is very pale bluish green. Crystals are transparent with vitreous to subadamantine luster. Eckhardite does not fluoresce under long- or short-wave ultraviolet light. The Mohs hardness could not be measured, but is estimated to be between 2 and 3, based upon the behavior of crystals when broken. The mineral is brittle with irregular fracture. Cleavage was not observed, but is likely on {101} based upon the crystal structure. The density could not be measured because it is greater than those of available high-density liquids and there is insufficient material for physical measurement. The calculated density based on the empirical formula and single-crystal cell is 4.644 g/cm³. Eckhardite crystals dissolve very slowly in cold, dilute HCl.

Because of the difficulty in working with the very thin needles and blades in high index of refraction liquids, the optical properties were determined using a combination of measurements and calculations: (1) the $2V$ was determined using extinction data with EXCALIBUR (Gunter et al. 2004); (2) the Becke line method was used to determine γ ; and (3) a Berek compensator was used to measure the retardation for $\gamma - \beta$ (0.035). The optical properties (white light) thus obtained are as follows: biaxial (-), $\alpha = 1.770$ (calc), $\beta = 1.860$ (calc), $\gamma = 1.895(5)$, $2V$ (meas.) = 61.2(5)°. The dispersion is $r < v$, perceptible, the optical orientation is $Z = b$; $X \approx [101]$, and the pleochroism is Z (light blue green) $< Y$ (very pale blue green) $< X$ (colorless).

RAMAN SPECTROSCOPY

Raman spectroscopic microanalyses were carried out using a Renishaw M1000 micro-Raman spectrometer system. Light from a 514.5 nm argon laser was focused onto the sample with a 100× objective lens. At 100% laser power the system provides ~5 mw of power at the sample, in a spot size of about 1 μ m. Peak positions were periodically calibrated against a silicon standard and rarely varied more than 1 cm⁻¹. All spectra were obtained with a dual-wedge polarization scrambler inserted directly above the objective lens to minimize the effects of polarization.

The sample used for the Raman spectra was the polished micro-probe sample. It consisted of a single ~40 μ m grain of eckhardite. Raman data were obtained at three spots, always starting at 10% power. Two of the spots gave high-quality, almost identical spectra, while one, although otherwise visually similar, had a poor signal-to-noise ratio. At one of the good spots the power was increased to 25%, then 50% without any change in the spectra other than the increased signal-to-noise ratio. The dominant features of the spectrum are features at 729 and 692 cm⁻¹ (Fig. 4). Tellurates have previously been shown to have the components of their ν_1 band in the 600 to 800 cm⁻¹ region (Blasse and Hordijk 1972; Frost 2009; Frost and Keeffe 2009). Also noteworthy is an O-H stretching feature centered near 3440 cm⁻¹ (Fig. 4, inset) that is an important confirmation of the presence of a hydrous component in the phase.

CHEMICAL COMPOSITION

Quantitative chemical analyses (4) of eckhardite were performed using a JEOL JXA-8200 electron microprobe at the Division of Geological and Planetary Sciences, California Institute of Technology. Analyses were conducted in WDS mode at 15 kV and 5 nA with a 1 μ m beam diameter. The small beam diameter was used because flat areas on the sample were limited and generally very small. The standards used were: galena (for Pb), anorthite

(for Ca), synthetic forsterite (for Mg), cuprite (for Cu), synthetic fayalite (for Fe), and Sb₂Te₃ (for Te). No other elements were detected by EDS analyses. Analytical results are given in Table 2. There was insufficient material for CHN analyses, so H₂O was calculated on the basis of 3 cations and 6 O apfu, as determined by the crystal-structure analysis (see below). Note that eckhardite is prone to electron beam damage, which contributes to the low analytical total. This is a common feature observed in almost all secondary hydrated tellurate species (e.g., Kampf et al. 2010a, 2010b, 2010c, 2010d, 2010e, 2010f, 2012, 2013a, 2013b; Mills et al. 2009, 2010).

The empirical formula (based on 6 O apfu) is Ca_{0.962}Pb_{0.073}Cu_{0.971}Mg_{0.005}Fe_{0.002}Te_{0.986}O₆H_{2.052}. The simplified formula is (Ca,Pb)Cu²⁺Te⁶⁺O₅(H₂O) and the end-member formula is CaCu²⁺Te⁶⁺O₅(H₂O), which requires CaO 17.03, CuO 24.16, TeO₃ 53.33, H₂O 5.47, total 100 wt% (see the crystal structure section for a discussion of the possible significance of Pb in the structure).

The Gladstone-Dale compatibility index 1 - (K_p/K_c) provides a measure of the consistency among the average index of refraction, calculated density, and chemical composition (Mandarino 2007). For eckhardite, the compatibility index is 0.020 based on the empirical formula, within the range of excellent compatibility.

X-RAY CRYSTALLOGRAPHY AND STRUCTURE DETERMINATION

All powder and single-crystal X-ray diffraction data were obtained on a Rigaku R-Axis Rapid II curved imaging plate microdiffractometer utilizing monochromatized MoK α radia-

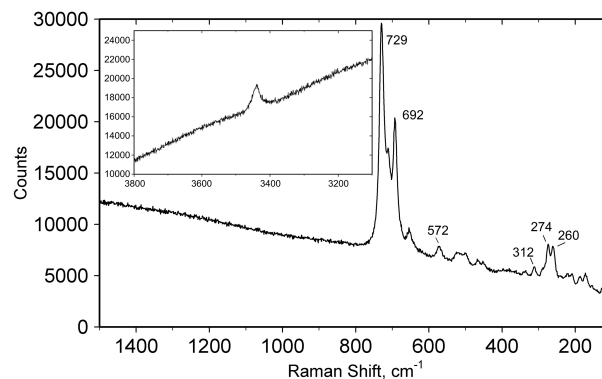


FIGURE 4. The Raman spectrum of eckhardite in the 1500–100 cm⁻¹ range that shows multiple features in the tellurate region with the two strongest lines at 692 and 729 cm⁻¹. In the 3800–3100 cm⁻¹ range (inset), an O-H stretching feature centered at about 3440 cm⁻¹ is consistent with the presence of H₂O.

TABLE 2. Chemical analytical data for eckhardite

Constituent	Average	Range	SD	Normalized wt%
PbO	4.54	4.19–4.74	0.24	4.79
CaO	15.09	14.99–15.19	0.12	15.90
MgO	0.06	0.02–0.10	0.04	0.06
CuO	21.59	21.20–22.15	0.40	22.74
Fe ₂ O ₃	0.05	0.02–0.12	0.04	0.06
TeO ₃	48.43	48.21–48.64	0.18	51.01
H ₂ O*	5.17			5.45
Total	94.93			100.01†

* Based on the crystal structure (3 cations and 6 O apfu).

† Rounding error.

tion. Observed powder d -values (with standard deviations) and intensities were derived by profile fitting using JADE 2010 software. Data (in angstroms) are given in Table 3. The observed powder data fit well with those calculated from the structure, also using JADE 2010. The unit-cell parameters refined from the powder data using JADE 2010 with whole-pattern fitting are: $a = 8.146(3)$, $b = 5.302(3)$, $c = 11.426(3)$ Å, $\beta = 101.807(7)^\circ$, and $V = 483.0(3)$ Å³. The differences between these cell parameters and those refined from the single-crystal data (Table 4) are attributable to the limitations of the whole-pattern-fitting method, particularly using MoK α radiation for a relatively low-symmetry structure with many closely spaced lines.

The Rigaku CrystalClear software package was used for processing of the diffraction data, including the application of an empirical multi-scan absorption correction using ABCOR (Higashi 2001). The structure was solved by direct methods using SIR2004 (Burla et al. 2005) and was refined using SHELXL-97 (Sheldrick 2008) employing neutral atom scattering factors.

Details concerning data collection and structure refinement are provided in Table 4. Fractional coordinates and atom displacement parameters are provided in Table 5, selected interatomic distances in Table 6, and bond valences in Table 7. (CIF¹ available on deposit.)

¹ Deposit item AM-13-813, CIFs and deposits. Deposit items are available two ways: For a paper copy contact the Business Office of the Mineralogical Society of America (see inside front cover of recent issue) for price information. For an electronic copy visit the MSA web site at <http://www.minsocam.org>, go to the *American Mineralogist* Contents, find the table of contents for the specific volume/issue wanted, and then click on the deposit link there.

TABLE 4. Data collection and structure refinement details for eckhardite

Diffractionmeter	Rigaku R-Axis Rapid II
X-ray radiation	MoK α ($\lambda = 0.71075$ Å)
Temperature	298(2) K
Structural formula	(Ca _{0.914} Pb _{0.086})Cu ²⁺ Te ⁶⁺ O ₅ (H ₂ O)
Space group	$P2_1/n$
Unit-cell dimensions	$a = 8.1606(8)$ $b = 5.3076(6)$ $c = 11.4412(15)$ Å $\beta = 101.549(7)^\circ$
Z	4
V	485.52(10) Å ³
Density (for above formula)	4.671 g/cm ³
Absorption coefficient	14.234 mm ⁻¹
$F(000)$	617.1
Crystal size	55 × 8 × 4 μm
θ range	3.64 to 25.01°
Index ranges	$-9 \leq h \leq 9$, $-6 \leq k \leq 6$, $-13 \leq l \leq 13$
Reflections collected/unique	2126/836 [$R_{int} = 0.078$]
Reflections with $F_o > 4\sigma F$	586
Completeness to $\theta = 25.01^\circ$	97.4%
Max., and min. transmission	0.9453 and 0.5082
Refinement method	Full-matrix least-squares on F^2
Parameters refined	84
GoF	1.116
Final R indices [$F_o > 4\sigma F$]	$R_1 = 0.0459$, $wR_2 = 0.0735$
R indices (all data)	$R_1 = 0.0824$, $wR_2 = 0.0863$
Extinction coefficient	0.0023(5)
Largest diff. peak/hole	+1.61/−1.65 e Å ⁻³

Notes: $R_{int} = \sum |F_o^2 - F_c^2(\text{mean})| / \sum [F_o^2]$.

GoF = $S = \{\sum [w(F_o^2 - F_c^2)^2] / (n - p)\}^{1/2}$.

$R_1 = \sum |F_o - |F_c|| / \sum |F_o|$.

$wR_2 = \{\sum [w(F_o^2 - F_c^2)^2] / \sum [w(F_o^2)^2]\}^{1/2}$.

$w = 1 / [\sigma^2(F_o^2) + (aP)^2 + bP]$ where a is 0, b is 11.8484, and P is $[2F_c^2 + \text{Max}(F_o^2, 0)]/3$.

TABLE 3. X-ray powder diffraction data for eckhardite

l_{obs}	d_{obs}	d_{calc}	l_{calc}	hkl	l_{obs}	d_{obs}	d_{calc}	l_{calc}	hkl
20	7.24(6)	7.2294	22	$\bar{1}01$	9	2.01(12)	2.0300	5	123
100	5.94(3)	5.9688	100	101	10	1.98(2)	1.9831	8	222
14	5.60(5)	5.6048	17	002			1.9569	3	214
27	4.79(2)	4.7970	19	011	12	1.92(2)	1.9269	11	024
37	4.415(18)	4.4220	27	110	10	1.90(3)	1.9039	6	411
12	3.98(4)	3.9977	7	200			1.8989	9	$\bar{3}21$
8	3.85(5)	3.8538	7	012	22	1.88(10)	1.8805	9	320
		3.6794	6	$\bar{1}03$			1.8167	4	223
28	3.64(24)	3.6751	4	$\bar{1}12$			1.8143	8	413
14	3.60(5)	3.6147	24	202	40	1.809(7)	1.8133	25	321
80	3.287(14)	3.2985	74	112			1.8073	4	404
33	3.203(17)	3.2093	31	$\bar{2}11$			1.7936	9	$\bar{1}16$
20	3.14(7)	3.1517	18	103	21	1.79(25)	1.7840	3	323
		3.0239	3	$\bar{1}13$			1.7737	4	402
		2.9876	6	$\bar{2}12$			1.7297	7	$\bar{1}25$
35	2.953(2)	2.9844	9	202	38	1.705(4)	1.7107	19	215
		2.9493	14	211			1.6565	4	116
		2.8024	4	004	9	1.625(9)	1.6311	4	132
17	2.711(13)	2.7182	13	301			1.5945	6	$\bar{1}33$
89	2.645(6)	2.6538	15	020			1.5903	8	415
8	2.578(20)	2.6455	53	$\bar{2}13$	25	1.589(3)	1.5891	5	$\bar{2}32$
		2.5824	7	021			1.5759	3	206
		2.4953	29	$\bar{1}14$			1.5598	7	413
48	2.485(7)	2.4834	12	301			1.5547	17	$\bar{5}12$
		2.4782	8	014	42	1.552(12)	1.5465	5	421
		2.4249	11	121			1.5428	6	133
36	2.414(9)	2.4098	7	$\bar{3}03$			1.5331	4	$\bar{2}17$
7	2.35(3)	2.3485	4	$\bar{3}12$	43	1.53(12)	1.5306	7	233
5	2.29(8)	2.2962	3	$\bar{2}14$			1.5258	4	406
		2.2806	5	$\bar{1}05$	4	1.51(4)	1.5129	10	$\bar{3}07$
46	2.245(8)	2.2568	25	114	6	1.50(19)	1.4998	4	134
		2.2450	10	122	5	1.48(22)	1.4828	4	331
		2.2163	6	$\bar{2}21$	4	1.47(3)	1.4747	4	422
14	2.20(4)	2.1942	8	$\bar{3}13$	6	1.45(6)	1.4530	4	234
7	2.134(16)	2.1392	5	$\bar{2}22$			1.4012	3	008
3	2.06(3)	2.0652	5	015	15	1.394(6)	1.3979	5	$\bar{1}35$

Note: Only calculated lines with intensities of 3 or greater are listed.

TABLE 5. Fractional coordinates, occupancies, and atom displacement parameters (\AA^2) for eckhardite

	x/a	y/b	z/c	U_{eq}	U_{11}	U_{22}	U_{33}	U_{23}	U_{13}	U_{12}
Ca*	0.2362(3)	0.9968(4)	0.3698(2)	0.0175(10)	0.0184(14)	0.0139(16)	0.0204(16)	0.0030(10)	0.0044(10)	0.0018(10)
Cu	0.8940(2)	0.5633(3)	0.23743(17)	0.0132(5)	0.0154(10)	0.0064(10)	0.0208(12)	0.0018(9)	0.0106(8)	0.0019(8)
Te	0.93390(11)	0.04791(18)	0.11673(9)	0.0099(3)	0.0120(5)	0.0063(5)	0.0133(6)	0.0005(5)	0.0073(4)	0.0003(4)
O1	0.7918(12)	0.3049(19)	0.0532(9)	0.014(2)	0.010(5)	0.020(6)	0.012(6)	0.006(5)	0.001(4)	0.002(5)
O2	0.0375(11)	0.2634(17)	0.2423(9)	0.011(2)	0.013(5)	0.009(5)	0.013(6)	-0.004(5)	0.010(5)	-0.001(4)
O3	0.0707(11)	0.7724(18)	0.1921(9)	0.011(2)	0.007(5)	0.014(6)	0.013(6)	-0.005(5)	0.008(4)	-0.006(4)
O4	0.7633(12)	0.8812(16)	0.1843(10)	0.014(2)	0.014(5)	0.006(5)	0.026(7)	0.004(5)	0.010(5)	0.001(4)
O5	0.1144(11)	0.153(2)	0.0322(10)	0.016(2)	0.009(5)	0.023(6)	0.016(6)	0.000(5)	0.004(5)	-0.002(4)
OW	0.0354(13)	0.756(2)	0.4495(11)	0.026(3)	0.024(6)	0.030(6)	0.024(7)	0.000(5)	0.009(6)	0.003(5)

* Refined occupancy of Ca:Pb = 0.914(4):0.086(4).

TABLE 6. Selected bond lengths (\AA) and angle ($^\circ$) in eckhardite

Ca-O1	2.310(10)	Cu-O4	1.960(9)	Te-O1	1.843(10)
Ca-O5	2.351(11)	Cu-O3	1.970(9)	Te-O2	1.898(10)
Ca-O3	2.360(9)	Cu-O2	1.971(9)	Te-O3	1.934(10)
Ca-OW	2.397(11)	Cu-O4	2.023(9)	Te-O4	1.936(9)
Ca-O2	2.411(10)	Cu-O1	2.513(11)	Te-O5	1.982(11)
Ca-O3	2.506(10)	Cu-OW	2.674(12)	Te-O5	1.997(9)
Ca-O2	2.746(9)	<Cu-O>	2.185	<Te-O>	1.932
<Ca-O>	2.440				
Hydrogen bonding					
OW...O1		2.676(15)			
OW...O4		3.035(17)			
O1...OW...O4		117.8(5)			

TABLE 7. Bond valence sums for eckhardite

	O1	O2	O3	O4	O5	OW	Σ
Ca _{0.914} Pb _{0.086}	0.40	0.31	0.35		0.36	0.32	2.11
		0.13	0.24				
Cu	0.10	0.45	0.46	0.47		0.07	1.94
				0.39			
Te	1.25	1.07	0.97	0.96	0.85		5.90
					0.81		
H	0.21					0.79	1.00
H'				0.08		0.92	1.00
Σ	1.96	1.96	2.02	1.90	2.02	2.10	

Notes: Values are expressed in valence units. Ca²⁺-O and Cu²⁺-O bond strengths are from Brown and Altermatt (1985); Pb²⁺-O bond strengths are from Krivovichev and Brown (2001); Te⁶⁺-O bond strengths are from Mills and Christy (2013); hydrogen-bond strengths, based on O...O bond lengths, are also from Brown and Altermatt (1985).

TABLE 8. Minerals with known structures that contain both essential Te⁶⁺ and Cu²⁺

agaite	Pb ₃ Cu ²⁺ Te ⁶⁺ O ₅ (OH) ₂ (CO ₃)	Kampf et al. (2013b)
bairdite	Pb ₂ Cu ²⁺ Te ⁶⁺ O ₁₀ (OH) ₂ (SO ₄)·H ₂ O	Kampf et al. (2013c)
eckhardite	(Ca,Pb)Cu ²⁺ Te ⁶⁺ O ₆ (H ₂ O)	This study
frankhawthorneite	Cu ₂ ²⁺ Te ⁶⁺ O ₄ (OH) ₂	Grice and Roberts (1995)
fuettererite	Pb ₃ Cu ₂ ²⁺ Te ⁶⁺ O ₆ (OH) ₂ Cl ₅	Kampf et al. (2013a)
housleyite	Pb ₆ Cu ²⁺ Te ⁶⁺ O ₁₈ (OH) ₂	Kampf et al. (2010b)
jensenite	Cu ₂ ²⁺ Te ⁶⁺ O ₆ ·H ₂ O	Grice et al. (1996)
khinite (-40 and -37)	PbCu ₃ ²⁺ Te ⁶⁺ O ₆ (OH) ₂	Hawthorne et al. (2009)
leisingite	Cu ₂ ²⁺ MgTe ⁶⁺ O ₆ ·6H ₂ O	Margison et al. (1997)
paratimroseite	Pb ₂ Cu ₂ ²⁺ (Te ⁶⁺ O ₆) ₂ (H ₂ O) ₂	Kampf et al. (2010e)
quetzalcoatlite	Zn ₆ Cu ₃ ²⁺ (Te ⁶⁺ O ₃) ₂ O ₆ (OH) ₆ (Ag,Pb) ₂ Cl _{4-2y} , x + y ≤ 2	Burns et al. (2000)
timroseite	Pb ₂ Cu ₂ ²⁺ (Te ⁶⁺ O ₆) ₂ (OH) ₂	Kampf et al. (2010e)

DESCRIPTION OF THE STRUCTURE

Eckhardite has a structure consisting of stair-step-like octahedral layers of Te⁶⁺O₆ and Cu²⁺O₆ octahedra parallel to {101}, which are linked in the [10 $\bar{1}$] direction by bonds to interlayer Ca atoms (Fig. 5). The layers (Fig. 6) can be described in terms of various types of linkages between and among the regular Te⁶⁺O₆ octahedra and Jahn-Teller distorted Cu²⁺O₆ octahedra. Taken separately, the TeO₆ octahedra link by edge sharing to form Te₂O₁₀ dimers and the CuO₆ octahedra link by corner sharing

across *cis*-edges to form chains parallel to [010]. Considered jointly, the Te₂O₁₀ dimers are joined by edge sharing with CuO₆ octahedra to create bands parallel to [010], which comprise each of the “stair-steps” of the sheet. The bands contain six-member rings of edge-sharing octahedra. The bands (or stair-steps) link to each other by corner sharing. The CaO₇ polyhedra, shown in ball-and-stick fashion in Figure 7, form edge-sharing chains along [010]. One apical O atom (OW) of the CuO₆ octahedron is a H₂O group. This OW vertex projects into the interlayer region, bonding to one Ca atom and extending hydrogen bonds to one O atom (O1) in the same layer and to one O atom (O4) in the next layer (Fig. 8).

In the structure refinement, the occupancy of the Ca site refined to (Ca_{0.914}Pb_{0.086}) in reasonable agreement with the empirical formula. The Ca site has a coordination of 7, with Ca-O bond lengths ranging from 2.310 to 2.746 \AA with the two longest bonds, 2.506 and 2.746 \AA , on the same side of the coordination polyhedron (Fig. 7). Despite the asymmetry of the bond distribution, which might be seen as benefiting partial occupancy by Pb²⁺ with stereoactive 6s² lone pair electrons, it is clear from the bond-valence summation (BVS) that the site strongly prefers occupancy by Ca; full occupancy by Ca would provide a BVS of 2.06 v.u., while full occupancy by Pb would provide a BVS of 2.76 v.u. Simply expanding the separation between the octahedral layers would seem to allow for the necessary increase in Ca-O bond lengths to permit the site to accommodate more Pb; however, in light of the presence of essential Pb in the other secondary minerals closely associated with eckhardite and the general rarity of Ca as an essential (or even minor) component in the secondary phases at Otto Mountain, it can be concluded that a Pb-dominant analog of eckhardite is probably not stable, at least in the conditions present in the Otto Mountain mineral assemblages. Nevertheless, the presence of 7–9% Pb in the Ca site appears to be significant, especially considering that bond-valence considerations indicate such a strong preference for Ca at the site. It is not clear whether: (1) the presence of Pb in the site merely reflects the abundance of Pb in the mineral-forming environment, in which case it might be argued that it has a destabilizing influence on the structure, or (2) the presence of a small amount of Pb in the Ca site may actually contribute to the stability of the structure in some way, although apparently not from a bond-valence perspective.

The only other mineral with a structure containing an edge-sharing dimer of TeO₆ octahedra [Te₂O₁₀] is thorneite, Pb₆(Te₂O₁₀)(CO₃)Cl₂(H₂O) (Kampf et al. 2010c); however, the structure of thorneite contains no Cu and the Te₂O₁₀ dimer links only to Pb polyhedra. All minerals with known structures containing

essential Te^{6+} and Cu^{2+} are listed in Table 8. All of these structures contain Te^{6+}O_6 octahedra and Cu^{2+}O_6 octahedra (or Cu^{2+}O_5 square pyramids). The most pertinent structural comparisons are to the minerals also containing large cations, i.e., Pb, and all such minerals, except quetzalcoatlite, occur in the mineral assemblages at Otto Mountain.

An interesting feature of the stair-step-like octahedral layers in eckhardite is that they are based upon hexagonal close packing (HCP), not only in terms of the individual steps (or bands) of edge-sharing octahedra, but even with respect to the continuous assembly of steps. The structure can be described as a stacking of stepped HCP layers alternating with chains of CaO_7 polyhedra. The structures of three other minerals containing Pb^{2+} , Te^{6+} , and Cu^{2+} in Table 7 are based on stair-step-like HCP polyhedral layers: bairdite, timroseite, and paratimroseite. However, the layers in these structures have a different polyhedral configuration than that in the eckhardite structure. The step-forming HCP bands in the structures of bairdite, timroseite, and paratimroseite are brucite-type sheet fragments, while that in the eckhardite structure is a gibbsite-type sheet fragment. Nevertheless, the HCP nature of the layers in all of these minerals is reflected in the similar cell dimensions along the lengths of the steps (eckhardite: $b = 5.3076$, bairdite: $b = 5.2267$, timroseite: $a = 5.2000$, and paratimroseite: $a = 5.1943$ Å). In Figure 5 the structures of eckhardite and bairdite are compared, and in Figure 6 the octahedral layers in these structures are compared.

ACKNOWLEDGMENTS

The paper benefited from comments by reviewers Mark Cooper and Sergey Krivovichev. The Caltech EMP analyses were supported by a grant from the Northern California Mineralogical Association and the Caltech spectroscopic work by NSF Grant EAR-0947956. The remainder of this study was funded by the John Jago Trelawney Endowment to the Mineral Sciences Department of the Natural History Museum of Los Angeles County.

REFERENCES CITED

- Blasse, G., and Hordijk, W. (1972) The vibrational spectrum of Ni_3TeO_6 and Mg_3TeO_6 . *Journal of Solid State Chemistry*, 5, 395–397.
- Brown, I.D., and Altermatt, D. (1985) Bond-valence parameters from a systematic analysis of the inorganic crystal structure database. *Acta Crystallographica*, B41, 244–247.
- Burla, M.C., Caliandro, R., Camalli, M., Carrozzini, B., Cascarano, G.L., De Caro, L., Giacovazzo, C., Polidori, G., and Spagna, R. (2005) SIR2004: An improved tool for crystal structure determination and refinement. *Journal of Applied Crystallography*, 38, 381–388.
- Burns, P.C., Pluth, J.J., Smith, J.V., Eng, P., Steele, I.M., and Housley, R.M. (2000) Quetzalcoatlite: New octahedral-tetrahedral structure from $2 \times 2 \times 40$ micron crystal at the Advanced Photon Source-GSE-CARS Facility. *American Mineralogist*, 85, 604–607.
- Frost, R.L. (2009) Tlapallite $\text{H}_6(\text{Ca,Pb})_2(\text{Cu,Zn})_3\text{SO}_4(\text{TeO}_3)_4\text{TeO}_6$, a multi-anion mineral: A Raman spectroscopic study. *Spectrochimica Acta Part A: Molecular and Biomolecular Spectroscopy*, 72, 903–906.
- Frost, R.L., and Keefe, E.C. (2009) Raman spectroscopic study of kuranakhite $\text{PbMn}^{4+}\text{Te}^{6+}\text{O}_6$ —A rare tellurate mineral. *Journal of Raman Spectroscopy*, 40, 249–252.
- Grice, J.D., and Roberts, A.C. (1995) Frankhawthorneite, a unique HCP framework structure of a cupric tellurate. *Canadian Mineralogist*, 33, 649–653.
- Grice, J.D., Groat, L.A., and Roberts, A.C. (1996) Jensenite, a cupric tellurate framework structure with two coordinations of copper. *Canadian Mineralogist*, 34, 55–59.
- Gunter, M.E., Bandli, B.R., Bloss, F.D., Evans, S.H., Su, S.C., and Weaver, R. (2004) Results from a McCrone spindle stage short course, a new version of EXCALIBUR, and how to build a spindle stage. *The Microscope*, 52, 23–39.
- Hawthorne, F.C., Cooper, M.A., and Back, M.E. (2009) Khinite-40 [= khinite] and khinite-3T [= parakhinite]. *Canadian Mineralogist*, 47, 473–476.
- Higashi, T. (2001) ABCOR. Rigaku Corporation, Tokyo, Japan.
- Housley, R.M., Kampf, A.R., Mills, S.J., Marty, J., and Thorne, B. (2011) The remarkable occurrence of rare secondary tellurium minerals at Otto Mountain near Baker, California—including seven new species. *Rocks and Minerals*, 86, 132–142.
- Kampf, A.R., Housley, R.M., Mills, S.J., Marty, J., and Thorne, B. (2010a) Lead-tellurium oxysalts from Otto Mountain near Baker, California: I. Ottoite, Pb_2TeO_5 , a new mineral with chains of tellurate octahedra. *American Mineralogist*, 95, 1329–1336.
- Kampf, A.R., Marty, J., and Thorne, B. (2010b) Lead-tellurium oxysalts from Otto Mountain near Baker, California: II. Housleyite, $\text{Pb}_2\text{CuTe}_4\text{TeO}_{18}(\text{OH})_2$, a new mineral with Cu-Te octahedral sheets. *American Mineralogist*, 95, 1337–1342.
- Kampf, A.R., Housley, R.M., and Marty, J. (2010c) Lead-tellurium oxysalts from Otto Mountain near Baker, California: III. Thorneite, $\text{Pb}_6(\text{TeO}_{10})(\text{CO}_3)\text{Cl}_2(\text{H}_2\text{O})$, the first mineral with edge-sharing octahedral dimers. *American Mineralogist*, 95, 1548–1553.
- Kampf, A.R., Mills, S.J., Housley, R.M., Marty, J., and Thorne, B. (2010d) Lead-tellurium oxysalts from Otto Mountain near Baker, California: IV. Markcooperite, $\text{Pb}_3(\text{UO}_2)\text{Te}^{6+}\text{O}_6$, the first natural uranyl tellurate. *American Mineralogist*, 95, 1554–1559.
- (2010e) Lead-tellurium oxysalts from Otto Mountain near Baker, California: V. Timroseite, $\text{Pb}_2\text{Cu}_2^{2+}(\text{Te}^{6+}\text{O}_6)_2(\text{OH})_2$, and paratimroseite, $\text{Pb}_2\text{Cu}_2^{2+}(\text{Te}^{6+}\text{O}_6)_2(\text{H}_2\text{O})_2$, new minerals with edge-sharing Cu-Te octahedral chains. *American Mineralogist*, 95, 1560–1568.
- (2010f) Lead-tellurium oxysalts from Otto Mountain near Baker, California: VI. Telluroperite, $\text{Pb}_2\text{Te}^{4+}\text{O}_4\text{Cl}_2$, the Te analogue of perite and nadorite. *American Mineralogist*, 95, 1569–1573.
- Kampf, A.R., Mills, S.J., Housley, R.M., Rumsey, M.S., and Spratt, J. (2012) Lead-tellurium oxysalts from Otto Mountain near Baker, California: VII. Chromschiefelinite, $\text{Pb}_{10}\text{Te}_8\text{O}_{20}(\text{CrO}_4)(\text{H}_2\text{O})_8$, the chromate analogue of schiefelinite. *American Mineralogist*, 97, 212–219.
- Kampf, A.R., Mills, S.J., Housley, R.M., and Marty, J. (2013a) Lead-tellurium oxysalts from Otto Mountain near Baker, California: VIII. Fuettererite, $\text{Pb}_3\text{Cu}_6^{2+}\text{Te}^{6+}\text{O}_6(\text{OH})_7\text{Cl}_5$, a new mineral with double spangolite-type sheets. *American Mineralogist*, 98, 506–511.
- (2013b) Lead-tellurium oxysalts from Otto Mountain near Baker, California: IX. Agaite, $\text{Pb}_3\text{Cu}^{2+}\text{Te}^{6+}\text{O}_5(\text{OH})_2(\text{CO}_3)$, a new mineral with CuO_5 - TeO_6 polyhedral sheets. *American Mineralogist*, 98, 512–517.
- Kampf, A.R., Mills, S.J., Housley, R.M., Rossman, G.R., Marty, J., and Thorne, B. (2013c) Lead-tellurium oxysalts from Otto Mountain near Baker, California: X. Bairdite, $\text{Pb}_2\text{Cu}_2^{2+}\text{Te}_2^{6+}\text{O}_{10}(\text{OH})_2(\text{SO}_4) \cdot \text{H}_2\text{O}$, a new mineral with thick HCP layers. *American Mineralogist*, 98, 1315–1321.
- Krivovichev, S.V., and Brown, I.D. (2001) Are the compressive effects of encapsulation an artifact of the bond valence parameters? *Zeitschrift für Kristallographie*, 216, 245–247.
- Mandarino, J.A. (2007) The Gladstone–Dale compatibility of minerals and its use in selecting mineral species for further study. *Canadian Mineralogist*, 45, 1307–1324.
- Margison, S.M., Grice, J.D., and Groat, L.A. (1997) The crystal structure of leisingite, $(\text{Cu,Mg,Zn})_2(\text{Mg,Fe})\text{TeO}_6 \cdot 6\text{H}_2\text{O}$. *Canadian Mineralogist*, 35, 759–763.
- Mills, S.J., and Christy, A.G. (2013) Revised values of the bond valence parameters for $\text{Te}^{\text{VI}}\text{O}_6$, $\text{Te}^{\text{VI}}\text{O}_5$ and $\text{Te}^{\text{IV}}\text{O}_4$. *Acta Crystallographica*, B69, 145–149.
- Mills, S.J., Kolitsch, U., Miyawaki, R., Groat, L.A., and Poirier, G. (2009) Joëlbreggerite, $\text{Pb}_2\text{Zn}_3(\text{Sb}^{5+}, \text{Te}^{6+})\text{As}_2\text{O}_{13}(\text{OH}, \text{O})$, the Sb^{5+} analogue of dugganite, from the Black Pine mine, Montana. *American Mineralogist*, 94, 1012–1017.
- Mills, S.J., Kampf, A.R., Kolitsch, U., Housley, R.M., and Raudsepp, M. (2010) The crystal chemistry and crystal structure of kuksite, $\text{Pb}_2\text{Zn}_3\text{Te}^{6+}\text{P}_2\text{O}_{14}$, and a note on the crystal structure of yafsoanite, $(\text{Ca,Pb})_2\text{Zn}(\text{TeO}_6)_2$. *American Mineralogist*, 95, 933–938.
- Sheldrick, G.M. (2008) A short history of *SHELX*. *Acta Crystallographica*, A64, 112–122.

MANUSCRIPT RECEIVED MARCH 6, 2013

MANUSCRIPT ACCEPTED APRIL 28, 2013

MANUSCRIPT HANDLED BY ANTON CHAKHMOURADIAN